PERGAMON

Pattern Recognition 34 (2001) 2283–2303

PATTERN RECOGNITION
THE JOURNAL OF THE PATTERN RECOGNITION SOCIETY

www.elsevier.com/locate/patcog

Least-squares orthogonal distances fitting of circle, sphere, ellipse, hyperbola, and parabola

Sung Joon Ahn[a,*], Wolfgang Rauh[a], Hans-Jürgen Warnecke[b]

[a]*Fraunhofer Institute for Manufacturing Engineering and Automation (IPA), Nobelstr. 12, 70569 Stuttgart, Germany*
[b]*Fraunhofer Society, Leonrodstr. 54, 80636 Munich, Germany*

Received 16 June 2000; accepted 12 September 2000

Abstract

The least-squares fitting minimizes the squares sum of error-of-fit in predefined measures. By the geometric fitting, the error distances are defined with the orthogonal, or shortest, distances from the given points to the geometric feature to be fitted. For the geometric fitting of circle/sphere/ellipse/hyperbola/parabola, simple and robust nonparametric algorithms are proposed. These are based on the coordinate description of the corresponding point on the geometric feature for the given point, where the connecting line of the two points is the shortest path from the given point to the geometric feature to be fitted. © 2001 Pattern Recognition Society. Published by Elsevier Science Ltd. All rights reserved.

Keywords: Orthogonal distance fitting; Circle fitting; Sphere fitting; Conic fitting; Orthogonal contacting condition; Singular value decomposition; Nonlinear least squares; Gauss–Newton iteration

1. Introduction

The fitting of geometric features to given 2D/3D points is desired in various fields of science and engineering (e.g. astronomy [1], physics [2], biology [3], quality control and metrology [4–7]). In particular, circle and conic are the most common geometric features for the application of image processing. In the past, fitting problems have usually been solved through the least-squares method (LSM) [1] with respect to effective implementation and acceptable computing costs. The main alternative methods for the detection and analysis of geometric features, are Hough transform [8–10] and the moment method [11–13].

LS fitting minimizes the squares sum of error-of-fit in predefined measures. There are two main categories of LS fitting problems for geometric features, algebraic and geometric fitting, and these are differentiated by their respective definition of the error distances involved [14–16]. By *algebraic fitting*, a geometric feature is described by implicit equation $F(\mathbf{x}, \mathbf{a}) = 0$ with the parameters vector $\mathbf{a} = (a_1, \ldots, a_q)$. The error distances are defined with the deviations of the implicit equation from the expected value (i.e. zero) at each given point. The nonequality of the equation indicates that the given point does not lie on the geometric feature (i.e., there is some error-of-fit). Most publications about the LS fitting of circle [2,17–24], and ellipse [3,15,25–36], have been concerned with the squares sum of algebraic distances or their modifications:

$$\sum_{i=1}^{m} e_i^2 = \sum_{i=1}^{m} [(x_i - x_c)^2 + (y_i - y_c)^2 - r^2]^2 \tag{1}$$

for the circle fitting, and

$$\sum_{i=1}^{m} e_i^2 = \sum_{i=1}^{m} (Ax_i^2 + 2Bx_i y_i + Cy_i^2 + 2Dx_i + 2Ey_i + F)^2 \tag{2}$$

for the conic fitting. In spite of the advantages in implementation and computing costs, algebraic fitting has

* Corresponding author. Tel.: + 49-711-970-1859; fax: + 49-711-970-1004.

E-mail addresses: sja@ipa.fhg.de (S.J. Ahn), wor@ipa.fhg.de (W. Rauh), warnecke@zv.fhg.de (H.-J. Warnecke).

PII: S0031-3203(00)00152-7

drawbacks in accuracy and in relation to the physical interpretation of the fitting parameters and errors [29,32,37]. The known disadvantages of algebraic fitting are [16,29,31–33,38]:

- its definition of error distances does not coincide with measurement guidelines;
- it is very difficult to test the reliability of the estimated fitting parameters;
- the fitting parameters are not invariant to the coordinate transformation (e.g. by ellipse fitting, a simple parallel translation of the given points causes changes not only in the center coordinates, but also in the axis lengths and angle of the ellipse);
- the estimated fitting parameters are biased;
- the fitting errors are unwillingly weighted;
- the fitting procedure sometimes ends in an unintended geometric feature (e.g. a hyperbola instead of an ellipse).

By *geometric fitting*, also known as best fitting, the error distances are defined with the orthogonal, or shortest, distances from the given points to the geometric feature to be fitted. Geometric fitting is possibly the only solution to all of the above problems of algebraic fitting. This geometric error measure has been used as the benchmark by the goodness-of-fit test of various error measures. Especially for ellipse fitting, the papers of Safaee-Rad et al. [29] and Rosin [31,32] provide a good overview of the various error definitions.

The geometric fittings of circle/sphere and ellipse/hyperbola/parabola, are nonlinear problems and must be solved with iteration. For the geometric fitting of circle/sphere, there are some well established methods [4,39–41]. On the other hand, the geometric fitting of ellipse/hyperbola/parabola has been attacked in the last few years and is being further developed. Gander et al. [39] have proposed a geometric ellipse fitting algorithm in parametric form, which has a large number of fitting parameters ($m+5$ unknowns by $2m$ equations from m measurement points). Consequently, it has an unnecessarily deteriorative performance of convergence. Furthermore, their algorithm cannot directly take the results of a circle fitting as the reasonable initial values for the iterative ellipse fitting, because of the singularity in their Jacobian, occurring when the two axes of ellipse have the same length. The paper of Cui et al. [42] describes a geometric ellipse fitting with a minimum variance estimator and parameter space decomposition technique. Späth's papers [43–45] describe geometric fitting algorithms in parametric form for ellipse/hyperbola/parabola. By Späth's ellipse fitting algorithm, it is also assumed that the two axis lengths of ellipse are different.

In this paper, we propose very simple and robust nonparametric algorithms for geometric fittings of circle/sphere and ellipse/hyperbola/parabola. Our algorithms are based on the coordinate description of the corresponding point on the geometric feature for a given point, where the connecting line of the two points is the shortest path from the given point to the geometric feature. For the geometric circle/sphere fitting, the corresponding point on the circle/sphere is definitely described with the circle/sphere parameters and with the given point. On the other hand, in the geometric ellipse/hyperbola/parabola fitting, the corresponding point on the ellipse/hyperbola/parabola is described only implicitly through the orthogonal contacting conditions. When the corresponding point on the geometric feature for the given point is definitely or implicitly known, we can derive the Jacobian matrix at this point and apply the iterative nonlinear least-squares method.

Section 2 describes the applied nonlinear LS fitting in a general form. In Section 3, we present an algorithm for the geometric fitting of circle/sphere in an n-dimensional space ($n \geqslant 2$). Sections 4 and 5 contain the geometric fitting of ellipse/hyperbola/parabola in greater detail. This paper ends with a conclusion and summary of our discussion.

2. Nonlinear least-squares fitting

Suppose that q parameters $\mathbf{a}$ are assumed to be related to the $p(\geqslant q)$ measurements $\mathbf{X}$ according to

$$\mathbf{X} = \mathbf{F}(\mathbf{a}) + \mathbf{e}, \tag{3}$$

where $\mathbf{F}$ represents some nonlinear continuously differentiable observation functions of $\mathbf{a}$, and $\mathbf{e}$ denotes errors with zero mean, whose influence is to be eliminated. The nonlinear least-squares estimate of $\mathbf{a}$ given $\mathbf{X}$ must minimize the performance index

$$\sigma_0^2 = [\mathbf{X} - \mathbf{F}(\hat{\mathbf{a}})]^{\mathrm{T}}[\mathbf{X} - \mathbf{F}(\hat{\mathbf{a}})]. \tag{4}$$

For convenience, the weighting matrix (or the noise covariance matrix) is chosen as an identity matrix. The existence of the unbiased optimal solution, which is generally nonlinear in the estimate of $\mathbf{a}$, can be referenced from elsewhere [46]. There are various methods for the numerical solution of the above nonlinear estimation problem. In this paper, we have chosen the Gauss–Newton iteration with initial parameters vector $\mathbf{a}_0$ and step-size parameter λ

$$\left.\frac{\partial \mathbf{F}}{\partial \mathbf{a}}\right|_{\mathbf{a}_k} \Delta\mathbf{a} = \mathbf{X} - \mathbf{F}(\mathbf{a}_k), \tag{5}$$

$$\mathbf{a}_{k+1} = \mathbf{a}_k + \lambda\Delta\mathbf{a}. \tag{6}$$

The matrix of partial derivatives appearing in Eq. (5) is the Jacobian matrix **J**

$$J_{ij} \equiv \frac{\partial F_i}{\partial a_j}. \tag{7}$$

For this type of numerical solution the user must supply the function values vector **F** and the Jacobian matrix **J**, of course, at the nearest corresponding points on the geometric feature from each given point. This is a necessary requirement for the least-squares orthogonal distances fitting to work with the performance index of Eq. (4). We can locate, without difficulty, the nearest point on a circle/sphere from a given point. Unfortunately, in the case of ellipse/hyperbola/parabola fitting, it is not easy to locate the nearest point on the ellipse/hyperbola/parabola from a given point. We compare the cases of circle/sphere and ellipse/hyperbola/parabola fitting in Sections 3–5. When the function values vector **F** and the Jacobian matrix **J** are provided, the Jacobian matrix can be decomposed by SVD [47,48].

$$\left.\frac{\partial \mathbf{F}}{\partial \mathbf{a}}\right|_{\mathbf{a}_k} = \mathbf{U}\mathbf{W}\mathbf{V}^{\mathrm{T}} \tag{8}$$

with $\mathbf{U}^{\mathrm{T}}\mathbf{U} = \mathbf{V}^{\mathrm{T}}\mathbf{V} = \mathbf{I}$, $\mathbf{W} = [\mathrm{diag}(w_1, \ldots, w_q)]$.

After a successful termination of the iteration procedure, along with the performance index σ_0^2 of Eq. (4), the information about the quality of the fitting parameters will be provided.

The parameter covariance matrix:

$$\mathrm{Cov}(\mathbf{a}) = (\mathbf{J}^{\mathrm{T}}\mathbf{J})^{-1} = (\mathbf{V}\mathbf{W}\mathbf{U}^{\mathrm{T}}\mathbf{U}\mathbf{W}\mathbf{V}^{\mathrm{T}})^{-1} = \mathbf{V}\mathbf{W}^{-2}\mathbf{V}^{\mathrm{T}},$$

thus

$$\mathrm{Cov}(a_j, a_k) = \sum_{i=1}^{q} \left(\frac{V_{ji}V_{ki}}{w_i^2}\right), \quad j = 1, \ldots, q, \quad k = 1, \ldots, q. \tag{9}$$

Consequently, the variance of the estimated parameters:

$$\sigma^2(a_j) = \frac{\sigma_0^2}{p-q}\mathrm{Cov}(a_j, a_j), \quad j = 1, \ldots, q \tag{10}$$

and the correlation coefficients:

$$\rho(a_j, a_k) = \frac{\mathrm{Cov}(a_j, a_k)}{\sqrt{\mathrm{Cov}(a_j, a_j)\mathrm{Cov}(a_k, a_k)}},$$
$$j = 1, \ldots, q, \quad k = 1, \ldots, q.$$

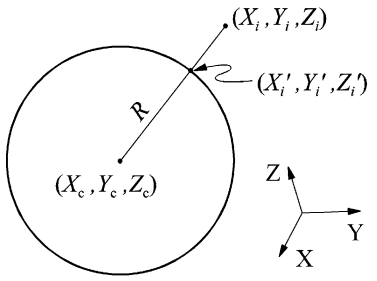

Fig. 1. A circle/sphere centered at $\mathbf{X}_c$ with radius R.

3. Geometric fitting of circle and sphere

The circle/sphere in an n-dimensional space ($n \geqslant 2$) with the center at $\mathbf{X}_c$ and radius R can be described as below (Fig. 1)

$$\|\mathbf{X} - \mathbf{X}_c\|^2 = R^2. \tag{11}$$

For a given point $\mathbf{X}_i (\neq \mathbf{X}_c)$, the nearest corresponding point $\mathbf{X}_i'$ on the circle/sphere is

$$\mathbf{X}_i' = \mathbf{X}_c + R\frac{\mathbf{X}_i - \mathbf{X}_c}{\|\mathbf{X}_i - \mathbf{X}_c\|}, \quad i = 1, \ldots, m \tag{12}$$

with the orthogonal error distances vector

$$\mathbf{X}_i'' = \mathbf{X}_i - \mathbf{X}_i' = [\|\mathbf{X}_i - \mathbf{X}_c\| - R]\frac{\mathbf{X}_i - \mathbf{X}_c}{\|\mathbf{X}_i - \mathbf{X}_c\|}. \tag{13}$$

From Eq. (12), the Jacobian matrix **J** for the Gauss–Newton iteration can be directly derived:

$$\mathbf{J}_{\mathbf{X}_i',\mathbf{a}} = \frac{\partial}{\partial \mathbf{a}}\left[\mathbf{X}_c + R\frac{\mathbf{X}_i - \mathbf{X}_c}{\|\mathbf{X}_i - \mathbf{X}_c\|}\right]$$
$$= \frac{\partial \mathbf{X}_c}{\partial \mathbf{a}} + \frac{\mathbf{X}_i - \mathbf{X}_c}{\|\mathbf{X}_i - \mathbf{X}_c\|}\frac{\partial R}{\partial \mathbf{a}} - \frac{R}{\|\mathbf{X}_i - \mathbf{X}_c\|}$$
$$\times\left[\mathbf{I} - \frac{(\mathbf{X}_i - \mathbf{X}_c)(\mathbf{X}_i - \mathbf{X}_c)^{\mathrm{T}}}{\|\mathbf{X}_i - \mathbf{X}_c\|^2}\right]\frac{\partial \mathbf{X}_c}{\partial \mathbf{a}}. \tag{14}$$

For example, in the case of sphere fitting ($n = 3$), if we define the parameters vector **a**

$$\mathbf{a}^{\mathrm{T}} = (R, \mathbf{X}_c^{\mathrm{T}}) = (R, X_c, Y_c, Z_c), \tag{15}$$

then we will have

$$\frac{\partial R}{\partial \mathbf{a}} = (1 \,|\, \mathbf{0}^{\mathrm{T}}) \quad \text{and} \quad \frac{\partial \mathbf{X}_{\mathrm{c}}}{\partial \mathbf{a}} = (\mathbf{0} \,|\, \mathbf{I}). \tag{16}$$

With the Jacobian matrix $\mathbf{J}_{\mathbf{X}_i',\mathbf{a}}$ of Eq. (14), and the error distances vector $\mathbf{X}_i''$ of Eq. (13) at each point $\mathbf{X}_i'$, we construct $p(=m\cdot n)$ linear equations for the m given n-dimensional points. In the case of sphere fitting ($n=3$, $p=3m$, $q=4$), the linear equations (5) look like

$$\begin{pmatrix} J_{X_1',R} & J_{X_1',X_c} & J_{X_1',Y_c} & J_{X_1',Z_c} \\ J_{Y_1',R} & J_{Y_1',X_c} & J_{Y_1',Y_c} & J_{Y_1',Z_c} \\ J_{Z_1',R} & J_{Z_1',X_c} & J_{Z_1',Y_c} & J_{Z_1',Z_c} \\ \vdots & \vdots & \vdots & \vdots \\ J_{X_m',R} & J_{X_m',X_c} & J_{X_m',Y_c} & J_{X_m',Z_c} \\ J_{Y_m',R} & J_{Y_m',X_c} & J_{Y_m',Y_c} & J_{Y_m',Z_c} \\ J_{Z_m',R} & J_{Z_m',X_c} & J_{Z_m',Y_c} & J_{Z_m',Z_c} \end{pmatrix} \begin{pmatrix} \Delta R \\ \Delta X_{\mathrm{c}} \\ \Delta Y_{\mathrm{c}} \\ \Delta Z_{\mathrm{c}} \end{pmatrix} = \begin{pmatrix} X_1'' \\ Y_1'' \\ Z_1'' \\ \vdots \\ X_m'' \\ Y_m'' \\ Z_m'' \end{pmatrix}. \tag{17}$$

The initial parameters vector, starting the Gauss–Newton iteration, may be supplied from an algebraic circle fitting. Since the above algorithm is very robust, we can also take the center of gravitation and the RMS central distances.

$$\mathbf{X}_{\mathrm{c}} = \bar{\mathbf{X}} = \frac{1}{m}\sum_{i=1}^{m} \mathbf{X}_i, \quad R = \sqrt{\frac{1}{m}\sum_{i=1}^{m} |\mathbf{X}_i - \bar{\mathbf{X}}|^2}. \tag{18}$$

For an experimental example of the geometric circle fitting, we have taken $m=6$ coordinate pairs ($n=2$) from Gander's paper (Table 1) [39], the initial parameters vector $\mathbf{a}_0$ from Eq. (18), and the step size $\lambda = 1.3$. After 9 Gauss–Newton steps for the norm of the terminal correction vector $\|\Delta\mathbf{a}\| = 5.4\times10^{-6}$, we have obtained $\sigma_0 = 1.1080$ (Fig. 2a, Table 2a and b). Table 2b reveals a strong anti-correlation between the radius R and the coordinate Y_{c} of the circle which is caused by the distribution of the given points. With the initial parameters vector from an algebraic circle fitting [17], and the step size $\lambda = 1.2$, the same estimations are reached after 8 Gauss–Newton steps for $\|\Delta\mathbf{a}\| = 3.6\times10^{-6}$ (Fig. 2b). Gander's algorithm [39] with the initial parameter

Table 1
Six coordinate pairs used for circle fitting [39]

X	1	2	5	7	9	3
Y	7	6	8	7	5	7

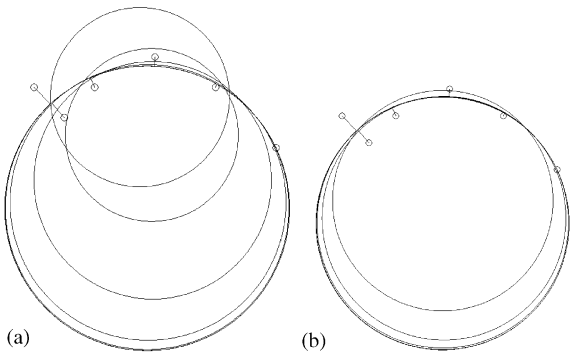

Fig. 2. Geometric circle fitting to the set of points in Table 1: (a) the center of gravitation and the RMS central distance are used as the initial parameter values; (b) the results of an algebraic circle fitting are used as the initial parameter values.

Table 2
(a) *Result of the circle fitting to the coordinate pairs in Table 1*

Parameters	R	X_{c}	Y_{c}	Iteration steps/$\|\Delta\mathbf{a}\|$
$\mathbf{a}_0$				
I	2.967	4.500	6.667	$9/5.4\times10^{-6}$
II	4.109	4.742	3.835	$8/3.6\times10^{-6}$
				$11/2.1\times10^{-6}$ (Gander)
				$116/1.0\times10^{-4}$ (Späth)
$\hat{\mathbf{a}}$	4.71423	4.73978	2.98353	$\sigma_0 = 1.1080$
$\sigma(\hat{\mathbf{a}})$	0.6595	0.2672	0.8274	

(b) *Correlation coefficients of the circle parameters in* (*a*)

$\rho(\hat{\mathbf{a}})$	R	X_{c}	Y_{c}
R	1.00		
X_{c}	−0.31	1.00	
Y_{c}	−0.97	0.34	1.00

values from an algebraic fitting, delivers the same estimations after 11 Gauss–Newton steps for $\|\Delta\mathbf{a}\| = 2.1\times10^{-6}$. Späth's algorithm [40] needed 116 iterations for $\|\Delta\mathbf{a}\| \approx 1.0\times10^{-4}$.

For an experimental comparison of geometric sphere fitting algorithms, we have taken $m = 8$ coordinate triples ($n = 3$) from Späth's paper (Table 3) [41], the initial parameters vector from an algebraic fitting [17], and the step size $\lambda = 1.0$. After 4 Gauss–Newton steps for $\|\Delta\mathbf{a}\| = 1.2\times10^{-6}$, we have obtained $\sigma_0 = 0.8832$ (Table 4). Späth's algorithm [41] needed 32 iterations for $\|\Delta\mathbf{a}\| \approx 1.0\times10^{-4}$.

For another set of 6 coordinate triples in Table 5 [41], we have taken the initial parameters vector from an algebraic fitting [17], and the step size $\lambda = 1.3$. After 9 Gauss–Newton steps for $\|\Delta\mathbf{a}\| = 5.3\times10^{-6}$, we have obtained $\sigma_0 = 1.1962$ (Table 6). Späth's algorithm [41] needed 150 iterations for $\|\Delta\mathbf{a}\| \approx 1.0\times10^{-4}$.

4. Geometric fitting of ellipse and hyperbola

In this section, we describe a new algorithm for geometric ellipse fitting. The geometric hyperbola fitting can be accomplished through a minimal modification of the geometric ellipse fitting. An ellipse in a plane can be uniquely described with 5 parameters, the center coordinates X_c, Y_c, axis lengths a, b ($a \geqslant b$), and pose angle α ($-\pi/2 < \alpha \leqslant \pi/2$) (see Fig. 3). For the least-squares orthogonal distances fitting of ellipse with the algorithm described in Section 2, we must locate the nearest corresponding point $\mathbf{X}_i'$ (orthogonal contacting point) on the ellipse for the given point $\mathbf{X}_i$, and evaluate the Jacobian matrix at $\mathbf{X}_i'$. To locate the points $\mathbf{X}_i'$ ($i = 1, \ldots, m$) on the ellipse, Gander et al. [39] and Späth [43] have introduced additional m unknown parameters, where each point $\mathbf{X}_i'$ has an individual angular parameter to be simultaneously estimated with the 5 ellipse parameters. As a consequence, their linear system has a bulky and sparse Jacobian matrix and shows only a deteriorative convergence. Both algorithms assume that the two axis lengths of ellipse are different. We have solved these problems of orthogonal contacting point and Jacobian matrix by introducing a temporary coordinate system xy positioned at (X_c, Y_c) and rotated with the angle α [29]. The use of the temporary coordinate system xy is not new at all, and very common for an ellipse fitting, but we exploit it as well as the orthogonal contacting conditions in order to derive the Jacobian $\mathbf{J}$ at the nearest corresponding points $\mathbf{X}_i'$ on the general rotated ellipse from the given points $\mathbf{X}_i$. We show the detailed procedures in the following subsections. The coordinate transformation between the two coordinate systems xy and XY is (Fig. 3)

$$\mathbf{x} = \mathbf{R}(\mathbf{X} - \mathbf{X}_c) \tag{19}$$

or

$$\mathbf{X} = \mathbf{R}^{-1}\mathbf{x} + \mathbf{X}_c, \tag{20}$$

where

$$\mathbf{R} = \begin{pmatrix} C & S \\ -S & C \end{pmatrix} \quad \text{and } \mathbf{R}^{-1} = \mathbf{R}^{\mathrm{T}},$$

$$\text{with } C = \cos\alpha, S = \sin\alpha. \tag{21}$$

4.1. Orthogonal contacting point on ellipse

In the xy coordinate system, the 3 of 5 ellipse parameters disappear (X_c, Y_c and α) and the ellipse will be

Table 3
Eight coordinate triples for sphere fitting [41]

X	0	−4	3	−1	−3	4	−2	−1
Y	−1	1	−3	−3	5	−1	1	−2
Z	5	−3	3	−3	−1	−1	−5	4

Table 5
Six coordinate triples for sphere fitting [41]

X	1	2	5	7	9	3
Y	1	2	3	4	5	6
Z	7	6	8	7	5	7

Table 4
Result of the sphere fitting to the coordinate triples in Table 3

Parameters	R	X_c	Y_c	Z_c	Iteration steps/$\|\Delta\mathbf{a}\|$
$\mathbf{a}_0$	5.152	−0.124	0.839	0.168	$4/1.2\times10^{-6}$ $32/1.0\times10^{-4}$ (Späth)
$\hat{\mathbf{a}}$	5.14973	−0.15433	0.87425	0.18060	$\sigma_0 = 0.8832$
$\sigma(\hat{\mathbf{a}})$	0.0862	0.1651	0.1764	0.1145	

Table 6
Result of the sphere fitting to the coordinate triples in Table 5

Parameters	R	X_c	Y_c	Z_c	Iteration steps/$\|\Delta\mathbf{a}\|$
$\mathbf{a}_0$	4.739	4.541	3.137	3.410	$9/5.3\times10^{-6}$ $150/1.0\times10^{-4}$(Späth)
$\hat{\mathbf{a}}$	5.60325	4.46679	3.27374	2.21017	$\sigma_0 = 1.1962$
$\sigma(\hat{\mathbf{a}})$	0.6912	0.3173	0.4964	0.8530	

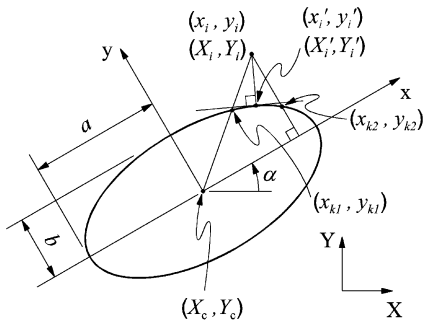

Fig. 3. An ellipse centered at (X_c, Y_c) with axis lengths a, b and angle α. The nearest point (X_i', Y_i') on the ellipse from a given point (X_i, Y_i) satisfies the orthogonal contacting conditions, and lies in the same quadrant of standard position as the given point.

described only with axis lengths a, b as below (standard position):

$$\frac{x^2}{a^2} + \frac{y^2}{b^2} = 1. \tag{22}$$

For a given point (x_i, y_i) in xy system, the tangent line at the orthogonal contacting point (x, y) on the ellipse, and the connecting line of the two points are perpendicular to each other:

$$\frac{dy}{dx}\cdot\frac{y_i - y}{x_i - x} = \frac{-b^2x}{a^2y}\cdot\frac{y_i - y}{x_i - x} = -1. \tag{23}$$

Rewrite Eqs. (22) and (23)

$$f_1(x, y) = \tfrac{1}{2}(a^2y^2 + b^2x^2 - a^2b^2) = 0 \tag{24}$$

and

$$f_2(x, y) = b^2x(y_i - y) - a^2y(x_i - x) = 0. \tag{25}$$

The orthogonal contacting point (x, y) on the ellipse must simultaneously satisfy Eqs. (24) and (25) (orthogonal contacting conditions). Safaee-Rad et al. [29] have combined two Eqs. (24) and (25) into one quartic equation and chosen one solution which has the shortest connecting line length among the maximum 4 real solutions. The numerical method solving this quartic equation is unstable, if $|x_i| \approx 0$ or $|y_i| \approx 0$. Thus, we have not combined two Eqs. (24) and (25) into one quartic, but have simultaneously solved these equations using the generalized Newton method as below:

$$\mathbf{Q} = \begin{pmatrix} \dfrac{\partial f_1}{\partial x} & \dfrac{\partial f_1}{\partial y} \\ \dfrac{\partial f_2}{\partial x} & \dfrac{\partial f_2}{\partial y} \end{pmatrix} = \begin{pmatrix} b^2x & a^2y \\ (a^2 - b^2)y + b^2y_i & (a^2 - b^2)x - a^2x_i \end{pmatrix}, \tag{26}$$

$$\mathbf{Q}_k\Delta\mathbf{x} = -\mathbf{f}(\mathbf{x}_k), \tag{27}$$

$$\mathbf{x}_{k+1} = \mathbf{x}_k + \Delta\mathbf{x}. \tag{28}$$

We supply the initial values $\mathbf{x}_0$ as below in Eq. (29), from the fact that the given point and its nearest corresponding point on the ellipse lie in the same quadrant of the standard position (see Fig. 3).

$$\mathbf{x}_0 = \tfrac{1}{2}(\mathbf{x}_{k1} + \mathbf{x}_{k2}), \tag{29}$$

where

$$\mathbf{x}_{k1} = \begin{pmatrix} x_i \\ y_i \end{pmatrix} ab/\sqrt{b^2x_i^2 + a^2y_i^2}$$

and

$$\mathbf{x}_{k2} = \begin{cases} \begin{pmatrix} x_i \\ \operatorname{sign}(y_i)\,\dfrac{b}{a}\sqrt{a^2 - x_i^2} \end{pmatrix} & \text{if } |x_i| < a, \\ \begin{pmatrix} \operatorname{sign}(x_i)a \\ 0 \end{pmatrix} & \text{if } |x_i| \geqslant a. \end{cases}$$

The iteration in Eqs. (27) and (28) with initial values $\mathbf{x}_0$ from Eq. (29) ends after 3–4 cycles providing adequately accurate coordinates for the orthogonal

contacting point. The Jacobian matrix $\mathbf{Q}$ in Eq. (26) is singular, if the given point $\mathbf{x}_i$ lies in the ellipse center and if the two axes of the ellipse have the same length. In other words, there is no unique orthogonal contacting point on a circle for the circle center.

After the given point $\mathbf{X}_i$ in XY system is transformed into $\mathbf{x}_i$ in xy system, using Eq. (19), the orthogonal contacting point $\mathbf{x}'_i$ will be found by the above generalized Newton method. Finally, we will have the point $\mathbf{X}'_i$ through a backward transformation of $\mathbf{x}'_i$ into XY system using Eq. (20). And the orthogonal error distances vector will be

$$\mathbf{X}''_i = \mathbf{X}_i - \mathbf{X}'_i. \tag{30}$$

4.2. Jacobian matrix at the orthogonal contacting point on ellipse

If we define the parameters vector $\mathbf{a}$

$$\mathbf{a} = (X_c, Y_c, a, b, \alpha)^T, \tag{31}$$

we get from the derivatives of coordinate transformation Eqs. (19) and (20):

$$\frac{\partial \mathbf{x}_i}{\partial \mathbf{a}} = \frac{\partial \mathbf{R}}{\partial \mathbf{a}}(\mathbf{X}_i - \mathbf{X}_c) - \mathbf{R}\frac{\partial \mathbf{X}_c}{\partial \mathbf{a}}$$

$$= \begin{pmatrix} -C & -S & 0 & 0 & y_i \\ S & -C & 0 & 0 & -x_i \end{pmatrix} \tag{32}$$

and

$$\mathbf{J}_{\mathbf{X}'_i,\mathbf{a}} = \left.\frac{\partial \mathbf{X}}{\partial \mathbf{a}}\right|_{\mathbf{X}=\mathbf{X}'_i} = \left.\left(\mathbf{R}^{-1}\frac{\partial \mathbf{x}}{\partial \mathbf{a}} + \frac{\partial \mathbf{R}^{-1}}{\partial \mathbf{a}}\mathbf{x} + \frac{\partial \mathbf{X}_c}{\partial \mathbf{a}}\right)\right|_{\mathbf{x}=\mathbf{x}'_i}$$

$$= \mathbf{R}^{-1}\left.\frac{\partial \mathbf{x}}{\partial \mathbf{a}}\right|_{\mathbf{x}=\mathbf{x}'_i} + \left.\begin{pmatrix} 1 & 0 & 0 & 0 & -xS & -yC \\ 0 & 1 & 0 & 0 & xC & -yS \end{pmatrix}\right|_{\mathbf{x}=\mathbf{x}'_i}. \tag{33}$$

The derivatives matrix $\partial\mathbf{x}/\partial\mathbf{a}$ appearing on the right hand side of Eq. (33) is to be derived from Eqs. (24), (25) and (32), since the point $\mathbf{x}'$ is only implicitly known through the orthogonal contacting conditions. We differentiate f_1 and f_2 of Eqs. (24) and (25) relatively to the parameters vector $\mathbf{a}$

$$\begin{pmatrix} \frac{\partial f_1}{\partial \mathbf{a}} \\ \frac{\partial f_2}{\partial \mathbf{a}} \end{pmatrix} = \begin{pmatrix} \frac{\partial f_1}{\partial X_c} & \frac{\partial f_1}{\partial Y_c} & \frac{\partial f_1}{\partial a} & \frac{\partial f_1}{\partial b} & \frac{\partial f_1}{\partial \alpha} \\ \frac{\partial f_2}{\partial X_c} & \frac{\partial f_2}{\partial Y_c} & \frac{\partial f_2}{\partial a} & \frac{\partial f_2}{\partial b} & \frac{\partial f_2}{\partial \alpha} \end{pmatrix} = \mathbf{0}. \tag{34}$$

After a series of substitutions and reductions in Eqs. (32)–(34), we will get

$$\mathbf{J}_{\mathbf{X}'_i,\mathbf{a}} = (\mathbf{R}^{-1}\mathbf{Q}^{-1}\mathbf{B})|_{\mathbf{x}=\mathbf{x}'_i}, \tag{35}$$

where $\mathbf{Q}$ is the Jacobian matrix as in Eq. (26), and

$$\mathbf{B} = (\mathbf{B}_1 \quad \mathbf{B}_2 \quad \mathbf{B}_3 \quad \mathbf{B}_4 \quad \mathbf{B}_5)$$

with

$$\mathbf{B}_1 = \begin{pmatrix} b^2xC - a^2yS \\ b^2(y_i - y)C + a^2(x_i - x)S \end{pmatrix},$$

$$\mathbf{B}_2 = \begin{pmatrix} b^2xS + a^2yC \\ b^2(y_i - y)S - a^2(x_i - x)C \end{pmatrix},$$

$$\mathbf{B}_3 = \begin{pmatrix} a(b^2 - y^2) \\ 2ay(x_i - x) \end{pmatrix},$$

$$\mathbf{B}_4 = \begin{pmatrix} b(a^2 - x^2) \\ -2bx(y_i - y) \end{pmatrix},$$

$$\mathbf{B}_5 = \begin{pmatrix} (a^2 - b^2)xy \\ (a^2 - b^2)(x^2 - y^2 - xx_i + yy_i) \end{pmatrix}. \tag{36}$$

4.3. Orthogonal distances fitting of ellipse

With the Jacobian matrix $\mathbf{J}_{\mathbf{X}'_i,\mathbf{a}}$ of Eq. (35), and the error distances vector $\mathbf{X}''_i$ of Eq. (30) at each point $\mathbf{X}'_i$, we construct $p(=2m)$ linear equations for the m given two-dimensional points. The linear equations (5) look like

$$\begin{pmatrix} J_{X'_1,X_c} & J_{X'_1,Y_c} & J_{X'_1,a} & J_{X'_1,b} & J_{X'_1,\alpha} \\ J_{Y'_1,X_c} & J_{Y'_1,Y_c} & J_{Y'_1,a} & J_{Y'_1,b} & J_{Y'_1,\alpha} \\ \vdots & \vdots & \vdots & \vdots & \vdots \\ J_{X'_m,X_c} & J_{X'_m,Y_c} & J_{X'_m,a} & J_{X'_m,b} & J_{X'_m,\alpha} \\ J_{Y'_m,X_c} & J_{Y'_m,Y_c} & J_{Y'_m,a} & J_{Y'_m,b} & J_{Y'_m,\alpha} \end{pmatrix} \begin{pmatrix} \Delta X_c \\ \Delta Y_c \\ \Delta a \\ \Delta b \\ \Delta \alpha \end{pmatrix}$$

$$= \begin{pmatrix} X''_1 \\ Y''_1 \\ \vdots \\ X''_m \\ Y''_m \end{pmatrix}. \tag{37}$$

The initial parameters vector starting the Gauss–Newton iteration may be supplied from an algebraic ellipse fitting, or from a circle fitting. The use of the results from

a circle fitting as the initial parameter values for iterative ellipse fitting is also recommended, since:

- The algebraic fitting of ellipses sometimes delivers obviously incorrect parameters.
- Circles are a special case of ellipses.
- Circle fitting is more robust than ellipse fitting, thus it guarantees a reasonable initial values set starting iterative ellipse fitting.

When the results from a circle fitting are to be used as the initial values for ellipse fitting, we set

$$(X_c, Y_c)_{\text{ellipse}} = (X_c, Y_c)_{\text{circle}}, \quad a = b = R, \text{ and } \alpha = 0. \tag{38}$$

If $a = b$ during iteration, the elements of $\mathbf{B}_5$ in Eq. (36) are all zero, and consequently, the last column of the Jacobian matrix in Eq. (37) will be filled with zeros. In other words, the parameter α is redundant for a circle. In this case, $\Delta\alpha$ will have the solution $\Delta\alpha = 0$ from SVD and subsequent backsubstitution in Eqs. (5) and (8) [48]. When $a < b$ after an updating of the parameters during iteration, we simply exchange the two values and set $\alpha \leftarrow \alpha - \text{sign}(\alpha)\pi/2$.

Table 7
Eight coordinate pairs used for ellipse fitting [39]

X	1	2	5	7	9	3	6	8
Y	7	6	8	7	5	7	2	4

For an experimental example of the ellipse fitting, we have taken 8 coordinate pairs in Table 7 [39], the initial parameters vector $\mathbf{a}_0$ from the geometric circle fitting, and the step size $\lambda = 1.2$. After 19 Gauss–Newton steps for the norm of the terminal correction vector $\|\Delta\mathbf{a}\| = 4.2 \times 10^{-6}$, we have obtained $\sigma_0 = 1.1719$ (Figs. 4a and b, Table 8a and b). Table 8b shows strong correlations between a and X_c, Y_c, caused by the distribution of the given points. For the initial parameter values from the algebraic conic fitting with the constraint of $F = 1$ in Eq. (2), the same final estimations are reached after 21 Gauss–Newton steps for $\|\Delta\mathbf{a}\| = 1.1 \times 10^{-6}$ (Figs. 4g and h). The comparable algorithm of Gander et al. [39] delivers the same estimations after 71 Gauss–Newton steps. Furthemore, they could not directly use the results of a circle fitting as the initial values for ellipse fitting because of the singularity in their Jacobian matrix by $a = b$. In order to bypass the singularity problem, they have used $a = R$, $b = R/2$. But generally said, an arbitrary modification of one parameter, without proper adjustments to the others, can cause a divergence!

In order to directly demonstrate the robust convergence of our algorithm, in comparison with Gander's, we have also tested the use of the initial values $a = R$, $b = R/2$ and $\alpha = 0$ from the geometric circle fitting. The final estimations are reached after 17 Gauss–Newton steps for the norm of the terminal correction vector $\|\Delta\mathbf{a}\| = 1.2 \times 10^{-6}$ (Figs. 4c and d). For another set of initial values $a = R$, $b = R/2$ and $\alpha = -1.211$, as this

Table 8
(a) *Result of the ellipse fitting to the coordinate pairs in Table 7*

Parameters	a	b	X_c	Y_c	α	Iteration steps/$\|\Delta\mathbf{a}\|$
$\mathbf{a}_0$						
I	3.391	3.391	4.840	4.797	0.000	$19/4.2 \times 10^{-6}$
II		3.391/2.0			0.000	$17/1.2 \times 10^{-6}$
III		3.391/2.0			−1.211	$23/5.2 \times 10^{-6}$
IV	3.880	2.896	4.918	5.006	−0.224	$21/1.1 \times 10^{-6}$
						$71/1.0 \times 10^{-6}$ (Gander)
$\hat{\mathbf{a}}$	6.51872	3.03189	2.69962	3.81596	0.35962	$\sigma_0 = 1.1719$
$\sigma(\hat{\mathbf{a}})$	3.9751	0.4750	3.2719	1.6488	0.1547	

(b) *Correlation coefficients of the ellipse parameters in* (*a*)

$\rho(\hat{\mathbf{a}})$	a	b	X_c	Y_c	α
a	1.00				
b	0.85	1.00			
X_c	−0.99	−0.87	1.00		
Y_c	−0.98	−0.92	0.98	1.00	
α	0.80	0.84	−0.79	−0.87	1.00

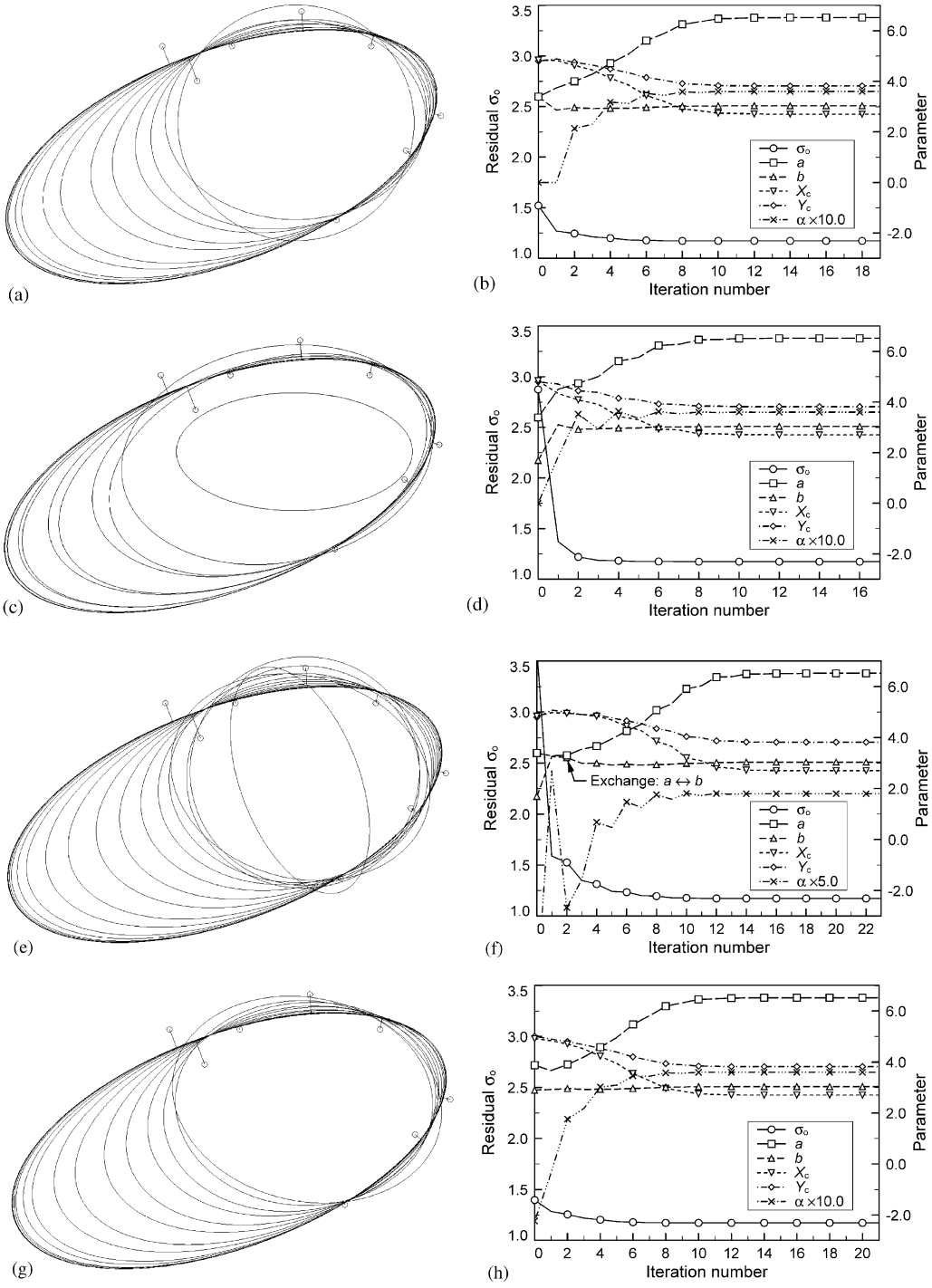

Fig. 4. Geometric ellipse fitting to the set of points in Table 7: (a) and (b) the results of the geometric circle fitting are used as the initial parameter values, $a = b = R$ and $\alpha = 0$; (c) and (d) $a = R$, $b = R/2$ and $\alpha = 0$; (e) and (f) $a = R$, $b = R/2$ and $\alpha = -1.211$; (g) and (h) the results of the algebraic conic fitting with the constraint of $F = 1$ in Eq. (2) are used as the initial parameter values.

was a worse initial values set, our algorithm needed 23 Gauss–Newton steps for $\|\Delta\mathbf{a}\| = 5.2\times10^{-6}$ (Figs. 4e and f).

Späth's algorithm [43] fits ellipses in normal positions ($\alpha = 0$ or $\pi/2$). In another paper [44], Späth has also considered additional constraints on the area of an ellipse. In order to directly compare the performance of our algorithm, we have inserted additional constraints on the angle and on the area of an ellipse into our algorithm. We simply modify the linear equations (5) as below, where w_3, w_4 are the constraint weighting factors with some large values:

$$f_3(\mathbf{a}) = \alpha - \text{const.} = 0, \tag{39}$$

$$f_4(\mathbf{a}) = ab - \text{const.} = 0, \tag{40}$$

$$\begin{pmatrix} \mathbf{J}_{\mathbf{X}_1,\mathbf{a}} \\ \vdots \\ \mathbf{J}_{\mathbf{X}_m,\mathbf{a}} \\ w_3\dfrac{\partial f_3(\mathbf{a})}{\partial \mathbf{a}} \\ w_4\dfrac{\partial f_4(\mathbf{a})}{\partial \mathbf{a}} \end{pmatrix}_{\mathbf{a}_k} \Delta\mathbf{a} = \begin{pmatrix} \mathbf{X}_1 - \mathbf{X}'_1 \\ \vdots \\ \mathbf{X}_m - \mathbf{X}'_m \\ -w_3 f_3(\mathbf{a}_k) \\ -w_4 f_4(\mathbf{a}_k) \end{pmatrix}. \tag{41}$$

For the set of 7 coordinate pairs in Table 9 [43], we have taken the initial parameters vector from the geometric circle fitting, the step size $\lambda = 1.2$, and the angular constraint and weighting $\alpha = \pi/2$, $w_3 = 1.0\times10^6$, respectively. After 9 Gauss–Newton steps for $\|\Delta\mathbf{a}\| = 7.8\times10^{-6}$, we have obtained $\sigma_0 = 1.5582$ (Fig. 5a, Table 10). Späth's algorithm [43] gives the same result after 32 iterations for $\|\Delta\mathbf{a}\| \approx 1.0\times10^{-4}$. With the constraints on angle and on area of $\alpha = 0$, $ab = 20$ with $w_3 = w_4 = 1.0\times10^6$, our algorithm delivers the final estimations where $\sigma_0 = 2.5525$ after 13 Gauss–Newton steps for $\|\Delta\mathbf{a}\| = 7.4\times10^{-6}$ (Figs. 5b and c, Table 11a and b). Table 11b shows a maximal anti-correlation between the axis lengths a and b while there is no correlation of the pose angle α with the other parameters which are caused by the constraints on the area and on the pose angle, respectively. Späth's algorithm [44] delivers the same result after 61 iterations for $\|\Delta\mathbf{a}\| \approx 1.0\times10^{-4}$.

For another set of 8 coordinate pairs in Table 12 [43], we have used the initial parameters vector from the geometric circle fitting, the step size $\lambda = 1.2$, and the angular constraint and weighting $\alpha = 0$, $w_3 = 1.0\times10^6$. After 10 Gauss–Newton steps for $\|\Delta\mathbf{a}\| = 4.7\times10^{-6}$, we

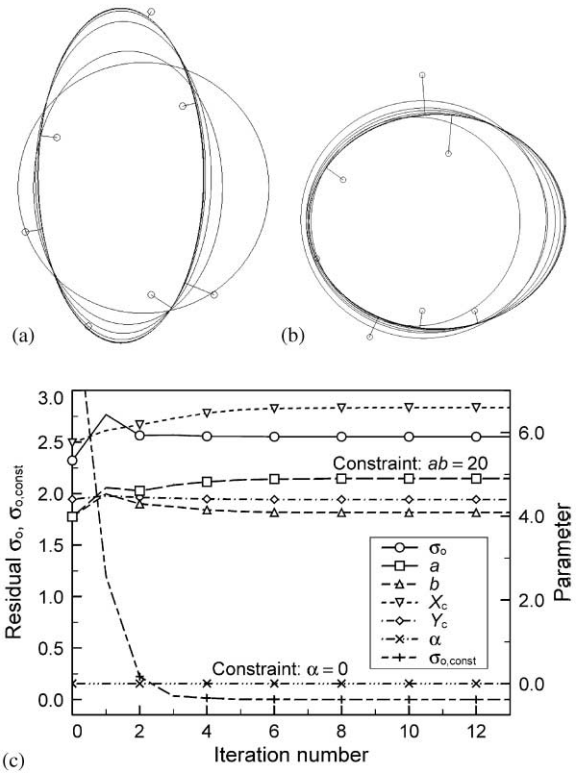

Fig. 5. Geometric ellipse fitting to the points set in Table 9: (a) with the angle constraint of $\alpha = \pi/2$; (b) and (c) with the angle and area constraints of $\alpha = 0$, $ab = 20$.

Table 9
Seven coordinate pairs used for ellipse fitting [43]

X	8	3	2	7	6	6	4
Y	1	6	3	7	1	10	0

Table 10
Result of the ellipse fitting to the coordinate pairs in Table 9

Parameters	a	b	X_c	Y_c	α	Iteration steps/$\|\Delta\mathbf{a}\|$	Constraints
$\mathbf{a}_0$	3.986	3.986	5.752	4.404	$\pi/2$	$9/7.8\times10^{-6}$ $32/1.0\times10^{-4}$ (Späth)	$\alpha - \pi/2 = 0$, $w = 1.0\times10^6$
$\hat{\mathbf{a}}$	5.32689	2.62537	5.04101	4.78989	1.57080	$\sigma_0 = 1.5582$	
$\sigma(\hat{\mathbf{a}})$	0.4628	0.2824	0.2228	0.3777	0.0000		

Table 11
(a) *Result of the ellipse fitting to the coordinate pairs in Table 9*

Parameters	a	b	X_c	Y_c	α	Iteration steps/$\|\Delta\mathbf{a}\|$	Constraints
$\mathbf{a}_0$	3.986	3.986	5.752	4.404	0.000	$13/7.4\times10^{-6}$ $61/1.0\times10^{-4}$ (Späth)	$\alpha=0$, $ab-20=0$,
$\hat{\mathbf{a}}$	4.89636	4.08467	6.59091	4.39588	0.00000	$\sigma_0=2.5525$	$w=1.0\times10^6$
$\sigma(\hat{\mathbf{a}})$	0.4323	0.3606	0.5910	0.3361	0.0000		

(b) *Correlation coefficients of the ellipse parameters in* (*a*)

$\rho(\hat{\mathbf{a}})$	a	b	X_c	Y_c	α
a	1.00				
b	−1.00	1.00			
X_c	0.38	−0.38	1.00		
Y_c	−0.06	0.06	−0.07	1.00	
α	−0.00	0.00	0.00	0.00	1.00

Table 12
Eight coordinate pairs used for ellipse fitting [43]

X	1	2	5	7	9	6	3	8
Y	7	6	8	7	5	7	2	4

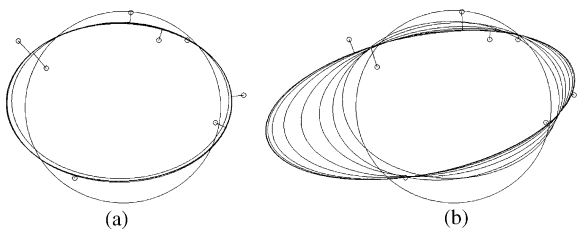

Fig. 6. Geometric ellipse fitting to the points set in Table 12: (a) with the angle constraint of $\alpha=0$; (b) without constraint.

have obtained $\sigma_0=1.3030$ (Fig. 6a, Table 13). Späth's algorithm gives the same result after 28 iterations for $\|\Delta\mathbf{a}\|\approx1.0\times10^{-4}$. Without any constraint for the same points set, our algorithm needed 14 Gauss–Newton steps for $\|\Delta\mathbf{a}\|=2.1\times10^{-6}$ and $\sigma_0=1.2049$ (Fig. 6b, Table 14).

All these experimental results show that our algorithm is very rigorous, and the use of the results of the geometric circle fitting is a good choice for the initial values for a geometric ellipse fitting.

4.4. Orthogonal distances fitting of hyperbola

A hyperbola in a plane can also be uniquely described with 5 parameters as the case of an ellipse, the center coordinates X_c, Y_c, axis lengths a, b, and pose angle $\alpha(-\pi/2<\alpha\leqslant\pi/2)$ (see Fig. 7). A hyperbola in standard position xy can be described as below:

$$\frac{x^2}{a^2}-\frac{y^2}{b^2}=1. \tag{42}$$

The only difference in comparison with an ellipse in standard position, is the sign of b^2, and thus, hints at the possibility of a simple modification of the ellipse fitting algorithm into a hyperbola fitting algorithm. What we have yet to do is, change the sign of b^2 in all deduced equations from Eq. (22), and supply proper initial values for the orthogonal contacting points and for the hyperbola parameters. In detail,

- allow a to be smaller than b;
- substitute each b^2 in Eqs. (23)–(26) and (36) with $-b^2$;
- substitute b of $\mathbf{B}_4$ in Eq. (36) with $-b$;
- instead of Eq. (29), use

$$\mathbf{x}_0=\begin{cases}\begin{pmatrix}\operatorname{sign}(x_i)a\\0\end{pmatrix} & \text{if } |x_i|\leqslant a,\\ \begin{pmatrix}x_i\\ \operatorname{sign}(y_i)\dfrac{b}{a}\sqrt{x_i^2-a^2}\end{pmatrix} & \text{if } |x_i|>a \text{ and } a\geqslant b,\\ \begin{pmatrix}\operatorname{sign}(x_i)\dfrac{a}{b}\sqrt{y_i^2+b^2}\\ y_i\end{pmatrix} & \text{if } |x_i|>a \text{ and } a<b\end{cases} \tag{43}$$

- as the initial parameter values for the iterative geometric hyperbola fitting, take the results of an algebraic conic fitting.

Späth's algorithm [43] fits hyperbola in a normal position ($\alpha=0$ or $\pm\pi/2$). For the purpose of a direct

Table 13
Result of the ellipse fitting to the coordinate pairs in Table 12

Parameters	a	b	X_c	Y_c	α	Iteration steps/$\|\Delta\mathbf{a}\|$	Constraints
$\mathbf{a}_0$	3.470	3.470	4.720	4.570	0.000	$10/4.7\times10^{-6}$ $28/1.0\times10^{-4}$ (Späth)	$\alpha=0$, $w=1.0\times10^{6}$
$\hat{\mathbf{a}}$	4.00931	2.85782	4.57351	4.74942	0.00000	$\sigma_0=1.3030$	
$\sigma(\hat{\mathbf{a}})$	0.2783	0.2410	0.2360	0.1997	0.0000		

Table 14
Result of the ellipse fitting to the coordinate pairs in Table 12

Parameters	a	b	X_c	Y_c	α	Iteration steps/$\|\Delta\mathbf{a}\|$
$\mathbf{a}_0$	3.470	3.470	4.720	4.570	0.000	$14/2.1\times10^{-6}$
$\hat{\mathbf{a}}$	5.58854	2.49072	3.53260	4.62307	0.20740	$\sigma_0=1.2049$
$\sigma(\hat{\mathbf{a}})$	1.7018	0.2170	1.2773	0.3377	0.0906	

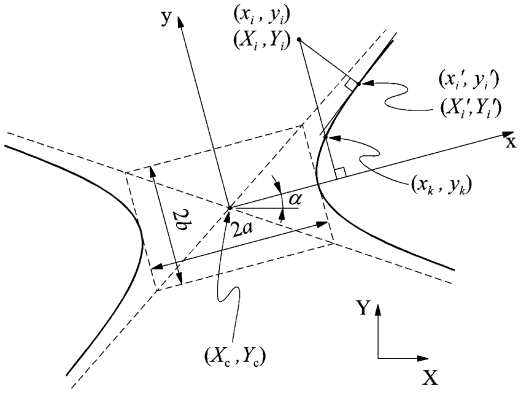

Fig. 7. A hyperbola centered at (X_c, Y_c) with axis lengths a, b and angle α. The nearest point (X_c', Y_c') on the hyperbola from a given point (X_i, Y_i) satisfies the orthogonal contacting conditions, and lies in the same quadrant of standard position as the given point.

comparison, if necessary, we additionally apply the angular constraint of Eq. (39) to our hyperbola fitting algorithm.

For the 8 coordinate pairs in Table 15 [43], we have used the initial parameters vector $\mathbf{a}_0$ from the algebraic conic fitting with the constraint of $A-C=1$ in Eq. (2), the step size $\lambda=1.0$, and the angular constraint and weighting $\alpha=0$, $w_3=1.0\times10^6$. After 8 Gauss–Newton steps for $\|\Delta\mathbf{a}\|=5.2\times10^{-6}$, we have obtained $\sigma_0=1.3151$ (Figs. 8a and b, Table 16a and b). Späth's algorithm [43] could not deliver a comparable result to our estimations even after about 100 iterations for $\sigma_0=1.8992$. In order to assess this questionable performance of Späth's algorithm, we have taken its estimation results as the initial values for our algorithm. After only 11 Gauss–Newton steps for $\|\Delta\mathbf{a}\|=1.4\times10^{-6}$, in comparison with about 100 iterations by Späth's algorithm, our final estimations where $\sigma_0=1.3151$ are reached (Figs. 8c and d). Without any constraint on the parameters, our algorithm needed 10 Gauss–Newton steps for $\|\Delta\mathbf{a}\|=8.9\times10^{-7}$ and $\sigma_0=1.0776$ (Fig. 8e, Table 17).

For another set of 8 coordinate pairs in Table 18 [43], we have used the initial parameters vector from the algebraic conic fitting, the step size $\lambda=1.0$, and the angular constraint and weighting $\alpha=0$, $w_3=1.0\times10^6$. After 5 Gauss–Newton steps for $\|\Delta\mathbf{a}\|=2.2\times10^{-7}$, we have obtained $\sigma_0=0.6064$ (Fig. 9, Table 19). Späth's algorithm [43] could only reach a two digit accuracy of our estimations after about 100 iterations for $\sigma_0=0.6071$. Using the result of Späth's algorithm as the initial values for our algorithm, after only 3 more Gauss–Newton steps for $\|\Delta\mathbf{a}\|=3.6\times10^{-6}$, our final estimations where $\sigma_0=0.6064$ are reached. Without any constraint, we needed 5 Gauss–Newton steps for $\|\Delta\mathbf{a}\|=2.6\times10^{-7}$ and $\sigma_0=0.6045$ (Table 20).

The robust convergence and the high accuracy of the estimated parameters by our hyperbola fitting algorithm are experimentally proven. Especially in direct comparisons with other algorithms, it demonstrated a superior performance.

5. Geometric fitting of parabola

The mathematical frame used for the geometric ellipse fitting in Section 4, including the derivatives of the coordinate transformation equation and of the orthogonal contacting condition equations relatively to the fitting

parameters, is generally applicable to the fitting of other geometric features in plane and space. In this section, we describe the geometric fitting of parabola as another application example of the proposed mathematical frame.

A parabola in a plane can be uniquely described with 4 parameters, the vertex coordinates X_c, Y_c, focus distance $p(>0)$ from directrix, and pose angle $\alpha(-\pi<\alpha\leqslant\pi)$ (Fig. 10). Analogously to the case of ellipse fitting, we use the temporary coordinate system xy centered at (X_c, Y_c) and rotated with the angle α.

5.1. Orthogonal contacting point and its Jacobian matrix

In the xy coordinate system, a parabola can be described with only one parameter, the focus distance p, as below:

$$y^2 = 2px. \tag{44}$$

In a similar way to the ellipse fitting, we derive the orthogonal contacting conditions:

$$f_5(x,y) = \tfrac{1}{2}(y^2 - 2px) = 0 \tag{45}$$

and

$$f_6(x,y) = y(x_i - x) + p(y_i - y) = 0. \tag{46}$$

Table 15
Eight coordinate pairs used for hyperbola fitting [43]

X	1	2	3	5	7	5	9	4
Y	4	2	6	6	−1	0	8	2

The orthogonal contacting point $\mathbf{x}_i'$ will be searched using a generalized Newton method as in Eqs. (27) and (28) with the Jacobian matrix

$$\mathbf{Q} = \begin{pmatrix} \dfrac{\partial f_5}{\partial x} & \dfrac{\partial f_5}{\partial y} \\ \dfrac{\partial f_6}{\partial x} & \dfrac{\partial f_6}{\partial y} \end{pmatrix} = \begin{pmatrix} -p & y \\ -y & x_i - x - p \end{pmatrix} \tag{47}$$

and with the initial starting point for iteration (Fig. 10)

$$\mathbf{x}_0 = \begin{cases} \mathbf{0} & \text{if } x_i < 0, \\ \begin{pmatrix} x_i \\ \operatorname{sign}(y_i)\sqrt{2px_i} \end{pmatrix} & \text{if } x_i \geqslant 0. \end{cases} \tag{48}$$

Now, if we arrange the parameters of parabola

$$\mathbf{a} = (X_c, Y_c, p, \alpha)^{\mathrm{T}}, \tag{49}$$

the derivatives of the coordinate transformation Eqs. (19) and (20) relatively to the parameters vector, will be

$$\frac{\partial \mathbf{x}_i}{\partial \mathbf{a}} = \begin{pmatrix} -C & -S & 0 & y_i \\ S & -C & 0 & -x_i \end{pmatrix} \tag{50}$$

and

$$\mathbf{J}_{\mathbf{X}_i',\mathbf{a}} = \mathbf{R}^{-1}\frac{\partial \mathbf{x}}{\partial \mathbf{a}}\bigg|_{\mathbf{x}=\mathbf{x}_i'} \begin{pmatrix} 1 & 0 & 0 & -xS & -yC \\ 0 & 1 & 0 & xC & -yS \end{pmatrix}\bigg|_{\mathbf{x}=\mathbf{x}_i'}. \tag{51}$$

Table 16
(a) *Result of the hyperbola fitting to the coordinate pairs in Table 15*

Parameters	a	b	X_c	Y_c	α	Iteration steps/$\|\Delta\mathbf{a}\|$	Constraints
$\mathbf{a}_0$							
I	1.218	0.620	−1.100	4.166	−0.107	$8/5.2\times10^{-6}$	$\alpha = 0$,
						$100/1.0\times10^{-4}$ (Späth)	$w = 1.0\times10^{6}$
II	0.748	0.537	1.154	3.338	0.000	$11/1.4\times10^{-6}$	
$\hat{\mathbf{a}}$	0.748	0.537	1.154	3.338	0.000	$\sigma_0 = 1.8992$ (Späth)	
	2.35016	1.10858	−1.66958	3.40627	0.00000	$\sigma_0 = 1.3151$	
$\sigma(\hat{\mathbf{a}})$	3.7699	1.4760	3.1904	0.1657	0.0000		

(b) *Correlation coefficients of the hyperbola parameters in* (*a*)

$\rho(\hat{\mathbf{a}})$	a	b	X_c	Y_c	α
a	1.00				
b	1.00	1.00			
X_c	−0.99	−0.98	1.00		
Y_c	0.35	0.35	−0.34	1.00	
α	−0.00	−0.00	0.00	−0.00	1.00

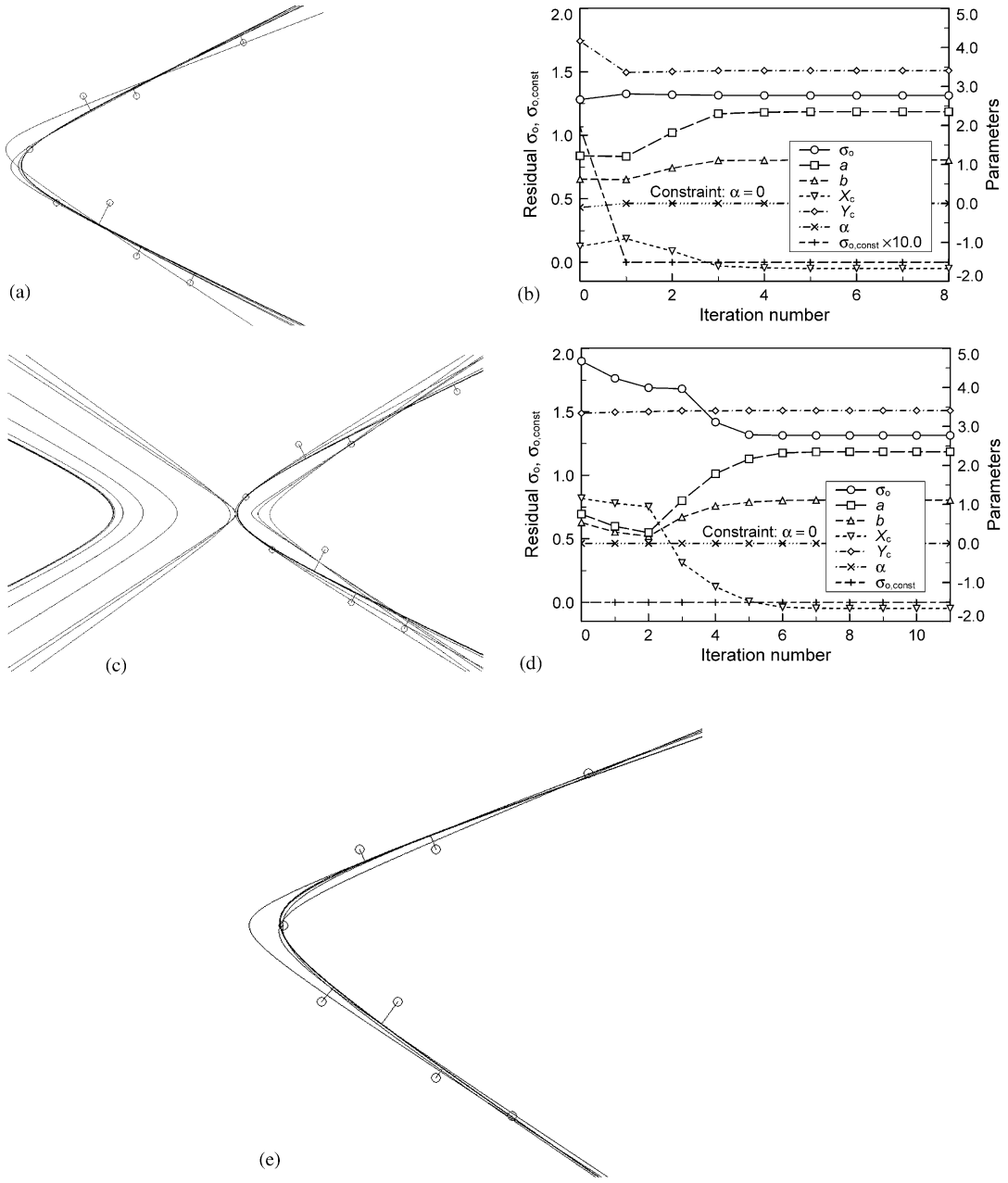

Fig. 8. Geometric hyperbola fitting to the set of points in Table 15 with the constraint of $\alpha = 0$: (a) and (b) the results of the algebraic conic fitting with the constraint of $A - C = 1$ for Eq. (2) are used as the initial parameter values; (c) and (d) the results of Späth's paper [43] are used as the initial parameter values; (e) free fitting without constraint.

From the derivatives of the orthogonal contacting condition equations f_5 and f_6 of (45) and (46) relatively to the parabola parameters, and using Eq. (50), we will get the derivatives matrix $\partial\mathbf{x}/\partial\mathbf{a}$ appearing on the right hand side of Eq. (51) as below:

$$\frac{\partial \mathbf{x}}{\partial \mathbf{a}} = \mathbf{Q}^{-1}\begin{pmatrix} 0 & 0 & x & 0 \\ yC - pS & yS + pC & y - y_i & -yy_i + px_i \end{pmatrix}, \quad (52)$$

Table 17
Result of the hyperbola fitting to the coordinate pairs in Table 15

Parameters	a	b	X_c	Y_c	α	Iteration steps/$\|\Delta\mathbf{a}\|$
$\mathbf{a}_0$	1.218	0.620	−1.100	4.166	−0.107	$10/8.9\times10^{-7}$
$\hat{\mathbf{a}}$	2.22229	1.11567	−1.28648	4.45735	−0.13217	$\sigma_0 = 1.0776$
$\sigma(\hat{\mathbf{a}})$	2.1997	0.8874	2.0269	0.4925	0.0531	

Table 18
Eight coordinate pairs used for hyperbola fitting [43]

X	−14	−8	−5	−4	5	6	9	13
Y	−4	7	5	2	4	1	0	−3

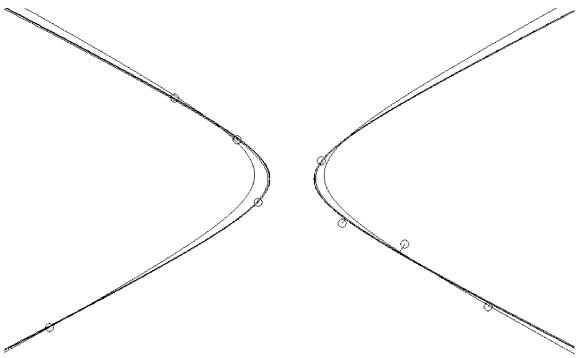

Fig. 9. Geometric hyperbola fitting to the set of points in Table 18 with the constraint of $\alpha = 0$.

where $\mathbf{Q}$ is the Jacobian matrix as in Eq. (47). Then, we have all necessary mathematical formulas for orthogonal contacting point and Jacobian matrix for the Gauss–Newton procedures described in Section 2. We now have to solve the practical problem of supplying initial parameter values for iterative fitting procedures.

5.2. Initial parameter values for geometric parabola fitting

Once the parameter values set $\{A,\ldots,F\}$ of the conic equation

$$f_7(x,y,A,B,C,D,E,F) = Ax^2 + 2Bxy + Cy^2 + 2Dx + 2Ey + F = 0 \tag{53}$$

is acquired through an algebraic conic fitting, we can refine it precisely for a parabola with the additional constraints of

$$B^2 - AC = 0 \quad \text{and} \quad A + C - 1 = 0. \tag{54}$$

Furthermore, if the pose angle of the parabola must be constrained, we must also consider

$$\frac{A}{\sqrt{A^2+B^2}} = \sin\alpha_{\text{constraint}} = c_1 \tag{55}$$

and

$$\frac{-B}{\sqrt{A^2+B^2}} = \cos\alpha_{\text{constraint}} = c_2$$

For a set of m given points, we search iteratively the 6 conic parameters under the constraints of Eqs. (54) and (55)

$$\begin{pmatrix} x_1^2 & 2x_1y_1 & y_1^2 & 2x_1 & 2y_1 & 1 \\ \vdots & \vdots & \vdots & \vdots & \vdots & \vdots \\ x_m^2 & 2x_my_m & y_m^2 & 2x_m & 2y_m & 1 \\ -w_8C & 2w_8B & -w_8A & 0 & 0 & 0 \\ w_9 & 0 & w_9 & 0 & 0 & 0 \\ w_{10}c_2^2 & w_{10}c_1c_2 & 0 & 0 & 0 & 0 \\ w_{10}c_1c_2 & w_{10}c_1^2 & 0 & 0 & 0 & 0 \end{pmatrix}_k \begin{pmatrix} \Delta A \\ \Delta B \\ \Delta C \\ \Delta D \\ \Delta E \\ \Delta F \end{pmatrix}$$

$$= \begin{pmatrix} -f_7(x_1,y_1,A,\cdots,F) \\ \vdots \\ -f_7(x_m,y_m,A,\cdots,F) \\ -w_8(B^2-AC) \\ -w_9(A+C-1) \\ -w_{10}(A-c_1\sqrt{A^2+B^2}) \\ -w_{10}(B+c_2\sqrt{A^2+B^2}) \end{pmatrix}_k, \tag{56}$$

where w_8, w_9 and w_{10} are the constraint weighting factors with some large values. After a successful termination of the parameter refining iteration, we obtain the 4 parabola parameter values [49] to be used as the starting values for the iterative procedures of geometric

Table 19
Result of the hyperbola fitting to the coordinate pairs in Table 18

Parameters	a	b	X_c	Y_c	α	Iteration steps/$\|\Delta\mathbf{a}\|$	Constraints
$\mathbf{a}_0$	4.647	2.479	0.497	3.300	−0.001	$5/2.2\times10^{-7}$	$\alpha=0$,
I						$100/1.0\times10^{-4}$ (Späth)	$w=1.0\times10^{6}$
II	4.015	2.024	0.612	3.125	0.000	$3\ /\ 3.6\times10^{-6}$	
$\hat{\mathbf{a}}$	4.015	2.024	0.612	3.125	0.000	$\sigma_0=0.6071$ (Späth)	
	4.04264	2.04223	0.60887	3.12768	0.00000	$\sigma_0=0.6064$	
$\sigma(\hat{\mathbf{a}})$	0.1668	0.1158	0.1102	0.0913	0.0000		

Table 20
Result of the hyperbola fitting to the coordinate pairs in Table 18

Parameters	a	b	X_c	Y_c	α	Iteration steps/$\|\Delta\mathbf{a}\|$
$\mathbf{a}_0$	4.647	2.479	0.497	3.300	−0.001	$5/2.6\times10^{-7}$
$\hat{\mathbf{a}}$	4.04353	2.04633	0.59623	3.13446	0.00202	$\sigma_0=0.6045$
$\sigma(\hat{\mathbf{a}})$	0.1730	0.1213	0.1241	0.0986	0.0076	

parabola fitting:

$$\begin{pmatrix} A & B \\ \dfrac{AD+2CD-BE}{A+C} & \dfrac{CE+2AE-BD}{A+C} \end{pmatrix}\begin{pmatrix} X_c \\ Y_c \end{pmatrix} = \begin{pmatrix} -\dfrac{AD+BE}{A+C} \\ -F \end{pmatrix}, \quad p=\frac{-(AE-BD)}{(A+C)\sqrt{A^2+B^2}},$$

$$\alpha=\tan^{-1}\left(\frac{A}{-B}\right). \tag{57}$$

Reversibly, from the parabola parameters, we will get the conic parameters:

$$\begin{aligned} A' &= \sin^2\alpha, \quad B' = -\sin\alpha\cos\alpha, \quad C' = \cos^2\alpha, \\ D' &= -X_c\sin^2\alpha + Y_c\sin\alpha\cos\alpha - p\cos\alpha, \\ E' &= X_c\sin\alpha\cos\alpha - Y_c\cos^2\alpha - p\sin\alpha, \\ F' &= (X_c\sin\alpha - Y_c\cos\alpha)^2 + 2p(X_c\cos\alpha + Y_c\sin\alpha). \end{aligned} \tag{58}$$

If $p<0$, we set $p\leftarrow -p$ and $\alpha\leftarrow\alpha-\mathrm{sign}(\alpha)\pi$, also during the Gauss–Newton iteration of Eqs. (5) and (6). We have observed in practice that the resulting parameter values set from the parameter refining iteration with Eqs. (54)–(56) provides a set of proper initial parameter values and guarantees a stable convergence of the Gauss–Newton iteration of Eqs. (5) and (6), when we have preconditioned the results of the algebraic conic fitting of Eq. (53) using Eqs. (57) and (58) successively before the start of the parameter refining iteration. In summary, we obtain the initial values set for the iterative parabola fitting in the following steps:

- Obtain 6 conic parameters from an algebraic conic fitting of Eq. (53).
- Condition the conic parameters using Eqs. (57) and (58) successively.

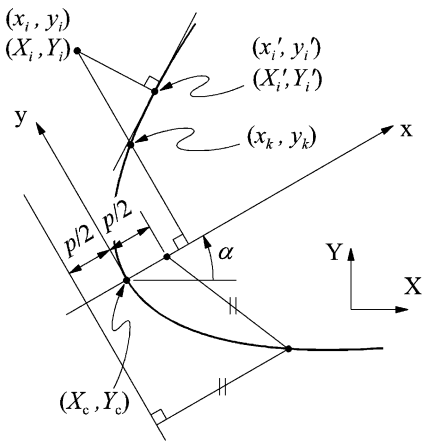

Fig. 10. A parabola with vertex at (X_c, Y_c), focus distance p, and pose angle α.

- Refine iteratively the conic parameters using Eqs. (54)–(56).
- Calculate the 4 parabola parameters from Eq. (57).

5.3. Experimental examples of orthogonal distances fitting of parabola

For the 5 coordinate pairs in Table 21 [45], we obtained the initial parameters vector $\mathbf{a}_0$ through the procedures described in the previous section with $w_8 = w_9 = 1.0 \times 10^6$ (without angular constraint). After 14 Gauss–Newton steps for $\|\Delta\mathbf{a}\| = 4.1 \times 10^{-6}$ with the step size $\lambda = 1.0$, we have obtained $\sigma_0 = 1.4086$ (Figs. 11a and b, Table 22).

Table 21
Five coordinate pairs used for parabola fitting [45]

X	−1	2	5	10	−4
Y	1	−2	3	−4	−3

To the same points set in Table 21, Späth's paper [45] fitted a parabola in normal position. For a direct comparison of our algorithm, we fix the pose angle at $\alpha_{\text{constraint}} = -\pi/2$. We obtained the initial parameters vector from the procedures in Section 5.2 using $w_8 = w_9 = w_{10} = 1.0 \times 10^6$. After 14 Gauss–Newton steps for $\|\Delta\mathbf{a}\| = 8.3 \times 10^{-6}$, $\lambda = 1.3$, with the angular constraint and weighting $\alpha = -\pi/2$ and $w_3 = 1.0 \times 10^6$, respectively (Eqs. (39) and (41)), we have obtained $\sigma_0 = 3.6821$ (Fig. 11c, Table 23). Späth's algorithm delivered the same results after about 100 iterations.

For another set of 6 coordinate pairs in Table 24 [45], we obtained the initial parameters vector from the

Table 22
Result of the parabola fitting to the coordinate pairs in Table 21

Parameters	p	X_c	Y_c	α	Iteration steps/$\|\Delta\mathbf{a}\|$
$\mathbf{a}_0$	0.512	−4.707	−1.269	0.088	$14/4.1 \times 10^{-6}$
$\hat{\mathbf{a}}$	0.38164	−6.73135	−1.30266	0.08523	$\sigma_0 = 1.4086$
$\sigma(\hat{\mathbf{a}})$	0.1764	3.5745	0.6159	0.0730	

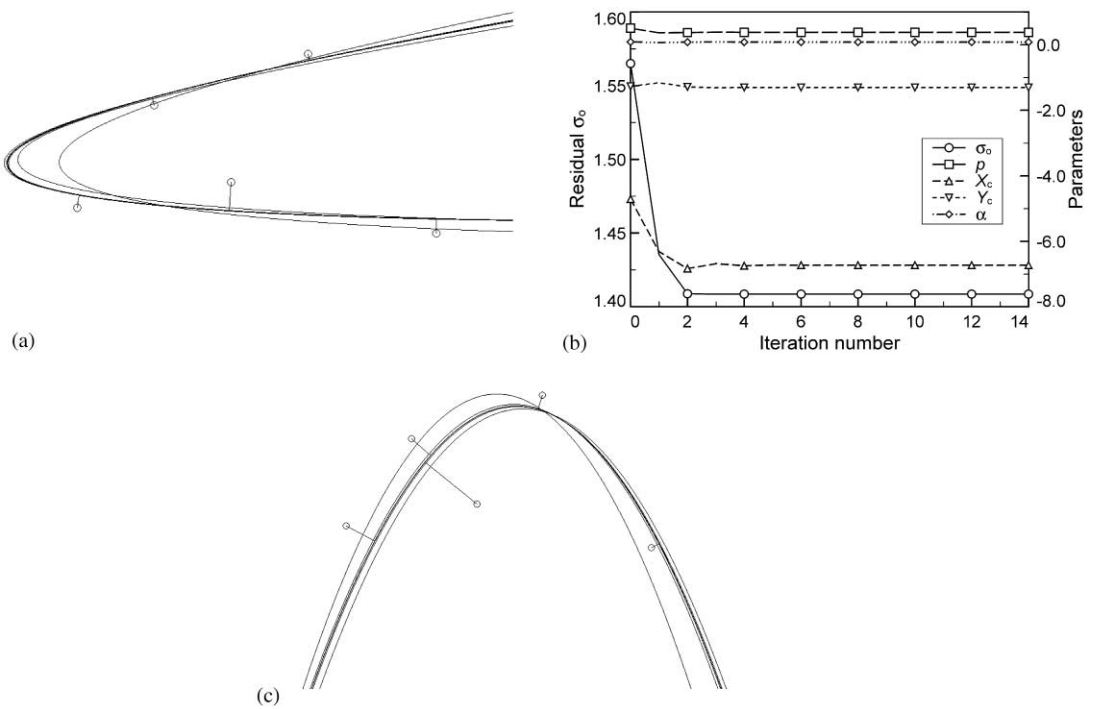

Fig. 11. Geometric parabola fitting to the set of points in Table 21: (a) and (b) free fitting without constraint; (c) with the constraint of $\alpha = -\pi/2$.

Table 23
Result of the parabola fitting to the coordinate pairs in Table 21

Parameters	p	X_c	Y_c	α	Iteration steps/$\|\Delta\mathbf{a}\|$	Constraints
$\mathbf{a}_0$	2.927	2.912	3.048	$-\pi/2$	$14/8.3\times10^{-6}$ $100/1.0\times10^{-4}$ (Späth)	$\alpha+\pi/2=0$, $w=1.0\times10^{6}$
$\hat{\mathbf{a}}$	3.40131	3.80624	2.49235	-1.57080	$\sigma_0=3.6821$	
$\sigma(\hat{\mathbf{a}})$	1.2533	0.8666	1.1827	0.0000		

Table 24
Six coordinate pairs used for parabola fitting [45]

X	-7	-3	0	1	1	0
Y	9	5	4	3	5	8

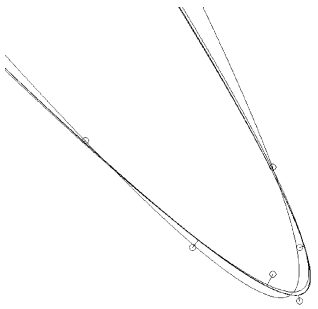

Fig. 12. Geometric parabola fitting to the set of points in Table 24.

algebraic parabola fitting of Section 5.2. After 7 Gauss–Newton steps for $\|\Delta\mathbf{a}\|=5.4\times10^{-6}$, we have obtained $\sigma_0=0.6881$ (Fig. 12, Table 25). Späth's algorithm [45] could only reach a two digit accuracy of our estimations. If we convert our results into the parameter format of Späth's paper (change the order of translation/rotation), we get $a=3.03178$, $b=1.79870$, $c=1.18495$. Späth's algorithm had $a=3.015$, $b=1.826$, $c=1.158$ where $\sigma_0=0.6888$.

6. Discussion and conclusions

We have proposed simple and robust nonparametric algorithms for the least-squares orthogonal distances fitting of circle/sphere and ellipse/hyperbola/parabola. For the geometric circle/sphere fitting, the Jacobian matrix at the nearest point on the circle/sphere from a given point is directly available from the circle/sphere parameters and the given point. The proposed circle/sphere fitting is very robust and we can simply take the center of gravitation and the RMS central distance as the initial parameter values. By the geometric ellipse/hyperbola/parabola fitting, the nearest point on the ellipse/hyperbola/parabola and the Jacobian matrix are not directly available. We have overcome these difficulties through the transformation of the ellipse/hyperbola/parabola into a standard position, and by utilizing the orthogonal contacting conditions. All necessary information for the iterative orthogonal distances fitting could be obtained from the derivatives of the coordinate transform equation, and of the orthogonal contacting equations. For ellipse fitting, the results from a circle fitting without modification can be used as the reasonable initial parameter values. Our experimental comparison with other geometric fitting algorithms shows that the proposed fitting algorithms have a superior performance in convergence, and in accuracy of the estimated parameters, both for geometric features in normal and rotated positions. Additionally, the parameter covariance matrix is immediately available with the termination of the iteration procedures, from which the reliability of the estimated parameters can be tested. If we would like to weight the given individual points, we multiply each row in Eq. (5),

Table 25
Result of the parabola fitting to the coordinate pairs in Table 24

Parameters	p	X_c	Y_c	α	Iteration steps/$\|\Delta\mathbf{a}\|$
$\mathbf{a}_0$	0.526	0.668	3.228	2.170	$7/5.4\times10^{-6}$
$\hat{\mathbf{a}}$	0.42196	1.21252	3.31011	2.25500	$\sigma_0=0.6888$ (Späth)
$\sigma(\hat{\mathbf{a}})$	0.0782	0.3102	0.2019	0.0476	$\sigma_0=0.6881$

for example, with the image gradient across the contour of the image object. In contrast to the algorithms of Gander, or of Späth, the memory space and computing costs of our algorithms are proportional to the number of the data points. In conclusion, the distinct features of the fitting algorithms presented in this paper are the derivatives of the coordinate transformation equation, and of the orthogonal contacting condition equations, relatively to the fitting parameters as in Eqs. (32)–(34) and (50)–(51), through which the orthogonal distances fitting could be made very simple, robust and comprehensible. The mathematical frame described in this paper for the orthogonal distances fitting is generally applicable to the other geometric fitting problems. Recently, we have extended the presented mathematical frame to the orthogonal distances fitting of three-dimensional surfaces and have successfully implemented it.

7. Summary

The fitting of geometric features to given 2D/3D points is desired in various fields of science and engineering. In particular, circle and conic are the most common geometric features for the application of image processing. In the past, the least-squares method (LSM) has often been applied to fitting of geometric features, and this method has proven its usability in effective implementation and acceptable computing costs. LS fitting minimizes the squares sum of error-of-fit in predefined measures. The two main categories of LS fitting problems for geometric features, algebraic and geometric fitting, are differentiated by their respective definition of the error distances. In spite of the advantages in implementation and computing costs, the *algebraic fitting* has drawbacks in accuracy and physical interpretation of the fitting parameters and errors. In *geometric fitting*, frequently cited as best fitting, the error distances are defined with the orthogonal, or shortest, distances from the given points to the geometric feature to be fitted. In this paper, we have proposed simple and robust algorithms for least-squares orthogonal distances fitting of circle/sphere in an n-dimensional space, and of ellipse/hyperbola/parabola in plane. The geometric fittings of circle/sphere and ellipse/hyperbola/parabola are nonlinear problems and must be solved with iteration. For the geometric fitting of circle/sphere, there are some well established methods. On the other hand, the geometric fitting of ellipse/hyperbola/parabola has been attacked since last few years and is being further developed. In this paper, we have proposed new algorithms of geometric fitting of circle/sphere and ellipse/hyperbola/parabola. Our algorithms are based on the coordinate description of the corresponding point on the geometric feature for a given point, where the connecting line of the two points is the shortest path from the given point to the geometric feature. By the geometric circle/sphere fitting, the corresponding point on the circle/sphere is definitely described with the circle/sphere parameters and with the coordinates of the given point. On the other hand, in the geometric ellipse/hyperbola/parabola fitting, the corresponding point on the ellipse/hyperbola/parabola is described only implicitly through the orthogonal contacting conditions, and the Jacobian matrix at this corresponding point are not directly available. We have overcome these difficulties through the transformation of ellipse/hyperbola/parabola into a standard position, and by utilizing the orthogonal contacting conditions. All necessary information for iterative orthogonal distances fitting could be obtained from the derivatives of the coordinate transform equation, and of the orthogonal contacting equations.

References

[1] C.F. Gauss, Theory of the Motion of the Heavenly Bodies Moving about the Sun in Conic Sections (Theoria motus corporum coelestium in sectionibus conicis solem ambientum) (First published in 1809, Translation by C.H. Davis), Dover, New York, 1963.
[2] N.I. Chernov, G.A. Ososkov, Effective algorithms for circle fitting, Comput. Phys. Commun. 33 (1984) 329–333.
[3] K.A. Paton, Conic sections in chromosome analysis, Pattern Recognition 2 (1970) 39–51.
[4] A. vom Hemdt, Standardauswertung in der Koordinatenmeßtechnik — Ein Beitrag zur Geometrieberechnung, Dissertation, RWTH Aachen, Germany, 1989.
[5] W. Rauh, Konturantastende und optoelektronicshe Koordinatenmeßgeräte für den industriellen Einsatz, Dissertation, Universität Stuttgart, Forschung und Praxis, No. 178, Springer, Berlin, 1993.
[6] M.L. Philpott, B.P. Welcher, D.R. Pankow, D. Vandenberg, A two phase circular regression algorithm for quantifying wear in CV joint ball race tracks, Wear 199 (2) (1996) 160–168.
[7] S.J. Ahn, M. Schultes, A new circular coded target for the automation of photogrammetric 3D-surface measurements, in: A. Gruen, H. Kahmen (Eds.), Optical 3-D Measurement Techniques IV, Herbert Wichmann Verlag, Heidelberg, 1997, pp. 225–234.
[8] P.V.C. Hough, Method and means for recognizing complex patterns, US Patent, No. 3 069 654, December 18, 1962.
[9] R.O. Duda, P.E. Hart, Use of the Hough transformation to detect lines and curves in pictures, ACM Commun. 15 (1) (1972) 11–15.
[10] D.H. Ballard, Generalizing the Hough transform to detect arbitrary shapes, Pattern Recognition 13 (2) (1981) 111–122.
[11] B.B. Chaudhuri, G.P. Samanta, Elliptic fit of objects in two and three dimensions by moment of inertia optimization, Pattern Recognition Lett. 12 (1991) 1–7.
[12] R. Safaee-Rad, K.C. Smith, B. Benhabib, I. Tchoukanov, Application of moment and Fourier descriptors to the accurate estimation of elliptical shape parameters, Pattern Recognition Lett. 13 (1992) 497–508.

[13] K. Voss, H. Süße, Invariant Fitting of Planar Objects by Primitives, IEEE Trans. PAMI 19 (1) (1997) 80–84.
[14] K. Pearson, On lines and planes of closest fit to systems of points in space, Philos. Mag. Ser. 6 2 (11) (1901) 559–572.
[15] P.D. Sampson, Fitting conic sections to "Very scattered" data: an iterative refinement of the Bookstein algorithm, CGIP 18 (1982) 97–108.
[16] DIN 32880-1, Coordinate Metrology; Geometrical Fundamental Principles, Terms and Definitions, German Standard, Beuth Verlag, Berlin, 1986.
[17] I. Kåsa, A circle fitting procedure and its error analysis, IEEE Trans. Instrum. Meas. 25 (1976) 8–14.
[18] T.J. Rivlin, Approximation by circles, in: G.G. Lorentz et. al. (Eds.), Approximation Theory II, Academic Press, New York, 1976, pp. 513–517.
[19] U.M. Landau, Estimation of a circular arc center and its radius, CVGIP 38 (1987) 317–326.
[20] R. Takiyama, N. Ono, A least square error estimation of the center and radii of concentric arcs, Pattern Recognition Lett. 10 (1989) 237–242.
[21] S.M. Thomas, Y.T. Chan, A simple approach for the estimation of circular arc center and its radius, CVGIP 45 (1989) 362–370.
[22] B.B. Chaudhuri, Optimal circular fit to objects in two and three dimensions, Pattern Recognition Lett. 11 (1990) 571–574.
[23] B.B. Chaudhuri, P. Kundu, Optimum circular fit to weighted data in multi-dimensional space, Pattern Recognition Lett. 14 (1993) 1–6.
[24] L. Moura, R. Kitney, A direct method for least-squares circle fitting, Comput. Phys. Commun. 64 (1991) 57–63.
[25] A. Albano, Representation of digitized contours in terms of conic arcs and straight-line segments, CGIP 3 (1974) 23–33.
[26] F.L. Bookstein, Fitting conic sections to scattered data, CGIP 9 (1979) 56–71.
[27] Y. Nakagawa, A. Rosenfeld, A note on polygonal and elliptical approximation of mechanical parts, Pattern Recognition 11 (1979) 133–142.
[28] J. Porrill, Fitting ellipses and predicting confidence envelopes using a bias corrected Kalman filter, Image Vision Comput. 8 (1) (1990) 37–41.
[29] R. Safaee-Rad, I. Tchoukanov, B. Benhabib, K.C. Smith, Accurate parameter estimation of quadric curves from grey-level images, CVGIP: Image Understanding 54 (2) (1991) 259–274.
[30] S. Chattopadhyay, P.P. Das, Parameter estimation and reconstruction of digital conics in normal positions, CVGIP: Graphical Models Image Process. 54 (5) (1992) 385–395.
[31] P.L. Rosin, A note on the least squares fitting of ellipses, Pattern Recognition Lett. 14 (1993) 799–808.
[32] P.L. Rosin, Assessing error of fit functions for ellipses, Graphical Models Image Process. 58 (5) (1996) 494–502.
[33] K. Kanatani, Statistical bias of conic fitting and renormalization, IEEE Trans. PAMI 16 (3) (1994) 320–326.
[34] J. Cabrera, P. Meer, Unbiased estimation of ellipses by bootstrapping, IEEE Trans. PAMI 18 (7) (1996) 752–756.
[35] A.W. Fitzgibbon, M. Pilu, R.B. Fisher, Direct least squares fitting of ellipses, Proceedings of the 13th International Conference on Pattern Recognition, Vienna, 1996, pp. 253–257.
[36] C. Chatterjee, E.K.P. Chong, Efficient algorithms for finding the centers of conics and quadrics in noisy data, Pattern Recognition 30 (5) (1997) 673–684.
[37] R.N. Goldman, Two approaches to a computer model for quadratic surfaces, IEEE Comput. Graphics Appl. 3 (9) (1983) 21–24.
[38] M. Berman, Large sample bias in least squares estimators of a circular arc center and its radius, CVGIP 45 (1989) 126–128.
[39] W. Gander, G.H. Golub, R. Strebel, Least-squares fitting of circles and ellipses, BIT 34 (1994) 558–578.
[40] H. Späth, Least-squares fitting by circles, Computing 57 (1996) 179–185.
[41] H. Späth, Least square fitting with spheres, J. Opt. Theory Appl. 96 (1) (1998) 191–199.
[42] Y. Cui, J. Weng, H. Reynolds, Estimation of ellipse parameters using optimal minimum variance estimator, Pattern Recognition Lett. 17 (1996) 309–316.
[43] H. Späth, Least-squares fitting of ellipses and hyperbolas, Comput. Stat. 12 (1997) 329–341.
[44] H. Späth, Orthogonal distance fitting by circles and ellipses with given area, Comput. Stat. 12 (1997) 343–354.
[45] H. Späth, Orthogonal squared distance fitting with parabolas, in: G. Alefeld, J. Herzberger (Eds.), Proceedings of the IMACS-GAMM International Symposium on Numerical Methods and Error-Bounds, University of Oldenburg, July 1995, Akademie-Verlag, Berlin, 1996, pp. 261–269.
[46] H.W. Sorenson, Parameter Estimation: Principles and Problems, Marcel Dekker, New York, 1980.
[47] G.H. Golub, C. Reinsch, Singular value decomposition and least squares solutions, Numer. Math. 14 (1970) 403–420.
[48] W.H. Press, B.P. Flannery, S.A. Teukolsky, W.T. Vetterling, Numerical Recipes in C: The Art of Scientific Computing, Cambridge University Press, Cambridge, UK, 1988.
[49] I.N. Bronštejn, K.A. Semendjajew, G. Musiol, H. Mühlig, Taschenbuch der Mathematik, 2nd Edition, Verlag Harri Deutsch, Thun, Germany, 1995, pp. 173–176.

About the Author—SUNG JOON AHN graduated with B.S. degree in Mechanical Design and Production Engineering from the Seoul National University in South Korea in 1985. He obtained his M.Sc. degree in Production Engineering from the Korea Advanced Institute of Science and Technology (KAIST) in 1987. He worked as a junior research scientist at the Research Center of LG Electronics, Ltd. in Seoul from 1987 to 1990. Since 1991 he has been working as a research scientist for the Fraunhofer Institute for Manufacturing Engineering and Automation (IPA) in Stuttgart, Germany. His research interests include pattern recognition, optical 3D-measurement, and camera calibration.

About the Author—WOLFGANG RAUH received his Doctorate in 1993 from the University of Stuttgart. He worked at the University of Stuttgart from 1984 until 1989 after having received his Diploma in Mechanical Engineering from the University of Karlsruhe in 1984.

He then became head of the group "Industrial Image Processing" at the Fraunhofer Institute for Manufacturing Engineering and Automation (IPA). In 1991 he was made head of the "Information Processing" department at the same institute. In this department, a wide variety of projects in the area of image processing are carried out.

About the Author—HANS-JÜRGEN WARNECKE, born 1934, studied Mechanical Engineering at Technical University of Braunshweig, Germany. He was Research Engineer at the Institute for Machine Tools and Manufacturing, afterwards, from 1965 to 1970, Managing Director for Planning and Manufacturing at the Rollei-Werke, Braunschweig, a camera factory. Since 1971 full Professor for Industrial Manufacturing and Management, University of Stuttgart and Head of the Fraunhofer Institute for Manufacturing Engineering and Automation (IPA) of the Fraunhofer Society for Applied Research. Main fields of research and development are management and organisation of industrial companies, computer integrated manufacturing, computer-aided planning of material flow, simulation, production planning and control, manufacturing processes, flexible manufacturing systems, industrial robots, automation of handling and assembly, quality control, industrial measurement, cleanroom manufacturing, semiconductor manufacturing automation, maintenance. About 10 books and many publications in the field of production, industrial engineering and automation. From October 1, 1993 President of the Fraunhofer Society, the largest institution for applied research and development in Europe with a budget of 1.4 billion DM, of which 500 million DM are proceeds from 3000 private and enterprises. 9000 employees in 50 institutes. In the years 1995–1997 President of VDI, the Association of German Engineers, the largest institution of this kind in Europe.